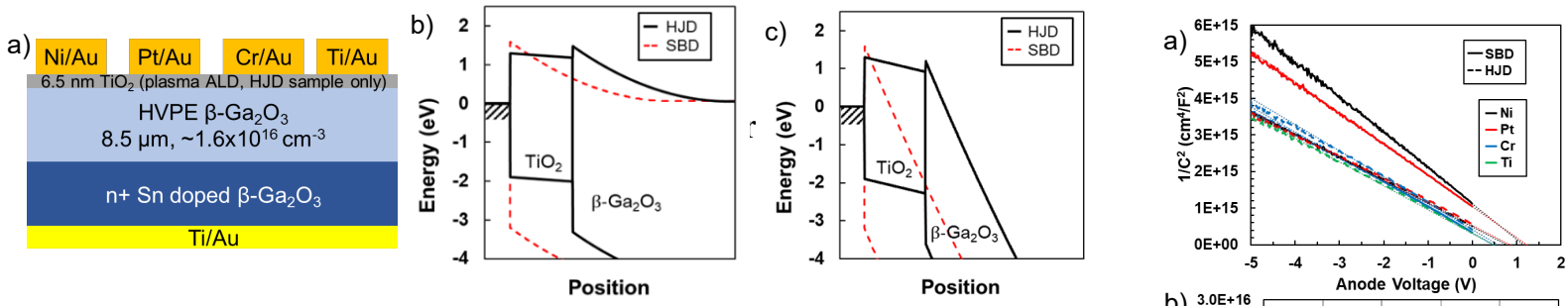

Figure 1: Schematics of a) the fabricated devices and the b) zero bias and c) reverse bias band diagrams of the SBD (red dash) and HJD (black).

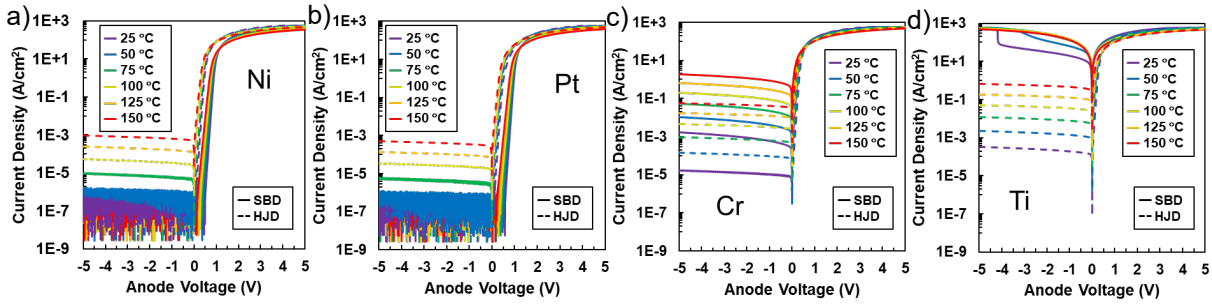

Figure 3: J-V-T data for a) Ni, b) Pt, c) Cr, and d) Ti SBDs (solid) and HJDs (dashed) from -5 to 5 V for 25 °C- 150 °C

Figure 2: a) $1/C^2$ versus voltage for all devices and b) extracted N_d-N_A versus depth.

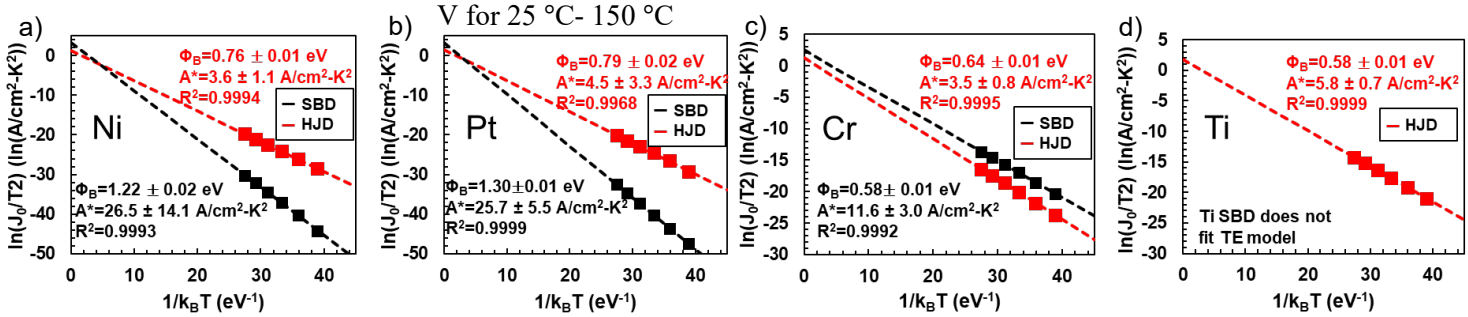

Figure 4: Richardson plots from J-V-T data for a) Ni, b) Pt, c) Cr, and d) Ti SBDs (black) and HJDs (red).

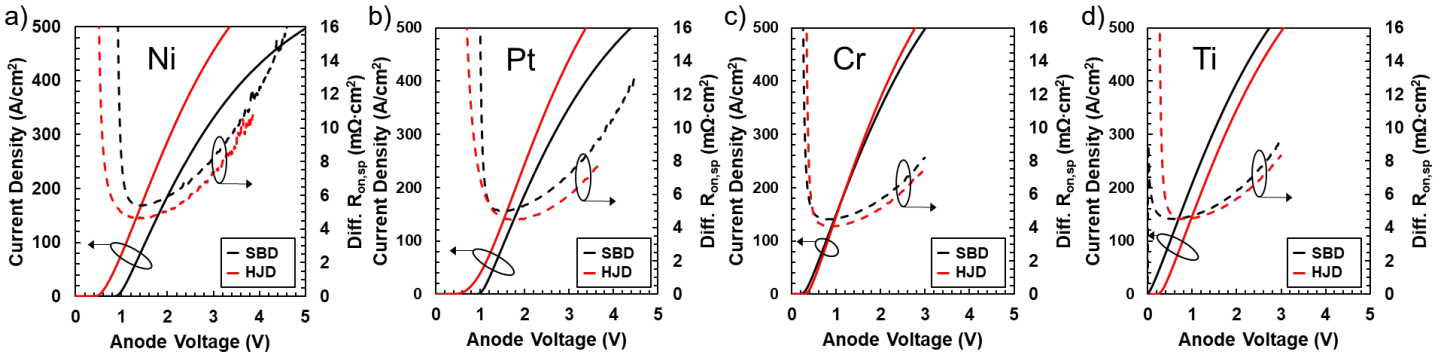

Figure 5: Linear scale forward J-V behavior of a) Ni, b) Pt, c) Cr, and d) Ti SBDs (black) and HJDs (red) with differential $R_{on,sp}$ in dashed lines.

Table 1: Extracted N_D-N_A, Φ_B and A* for all devices.

Device	N_d-N_A x10^{16} cm^{-3}	C-V Φ_B eV	J-V-T Φ_B eV	A* A/cm^2-K^2
Ni SBD	1.17	1.00	1.22	26.5
Pt SBD	1.34	1.23	1.30	25.7
Cr SBD	1.65	0.34	0.54	11.6
Ti SBD	N/A	N/A	N/A	N/A
Ni HJD	1.80	0.64	0.76	3.6
Pt HJD	1.83	0.72	0.79	4.5
Cr HJD	1.58	0.42	0.64	3.5
Ti HJD	1.75	0.34	0.58	5.8

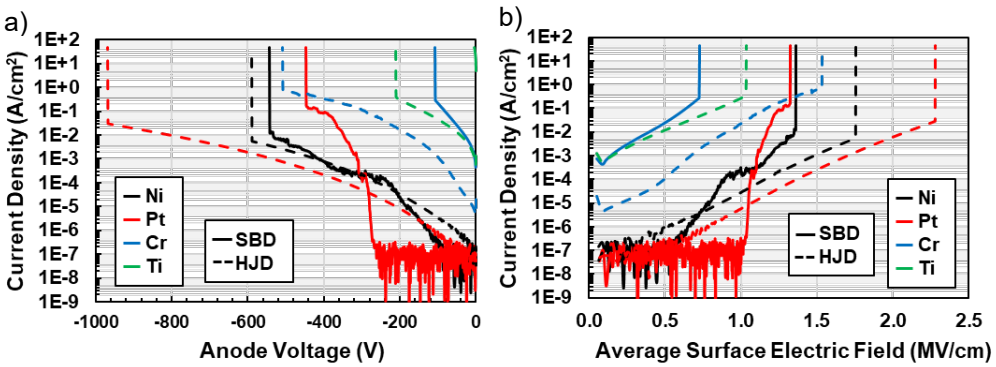

Figure 6: Reverse bias current behavior for all devices tested versus a) reverse voltage and b) average surface electric field (Ti SBD not shown).